hiPSC-derived 3D cardiac microtissue models with integrated immune cells and vasculature

Arslan-van Bergen, U.

Enhanced endothelial cell-cardiomyocyte crosstalk in hiPSC-derived vascularized 3D cardiac microtissues on chip through paracrine signalling

Authors and Affiliations

Ulgu Arslan[1], Marcella Brescia[1], Viviana Meraviglia[1], Dennis M. Nahon[1], Ruben W.J. van Helden[1], Jeroen M. Stein[1], Francijna E. van den Hil[1], Berend J. van Meer[1], Marc Vila Cuenca1[1,2], Christine L. Mummery[1], Valeria V. Orlova[1]*

[1]Department of Anatomy and Embryology, Leiden University Medical Centre, 2333ZC Leiden, The Netherlands

[2]Department of Clinical Genetics, Leiden University Medical Center, 2333ZA Leiden, the Netherlands

* Corresponding author

This work was combined with the study in chapter 5 and published in Stem Cell Reports, 2023 Jul 11, 18:1394–1404.
DOI: 10.1016/j.stemcr.2023.06.001.

Summary

The heart is one of the most metabolically active organs in the body. Vasculature is essential to provide selective nutrient delivery to meet its energy demand. In chapter 5, we developed an *in vitro* model of hiPSC-derived vascularized and perfusable cardiac microtissue on chip (VMToC). Here, we further characterized VMToCs function in more detail and investigated sarcomere organization and contractility. Vascularization improved endothelial cell (EC)-cardiomyocyte (CM) communication via EC-derived paracrine factors, such as nitric oxide (NO) and resulted in an enhanced inflammatory response. The platform sets the stage for studies on how organ-specific EC barriers respond to drugs or inflammatory stimuli.

Keywords:

human induced pluripotent stem cells; cardiac microtissue; heart-on-chip.

Introduction

The heart is highly vascularized. The crosstalk between vasculature and the myocardium ensures proper structure and function of the heart through the delivery of oxygen, nutrients and (blood) cells and removal of waste. Interruptions in this crosstalk have been implicated in cardiovascular disorders which are the major cause of death globally (Berry and Duncker, 2020). Several 3D microphysiological models of the human heart have been described in which cardiac stromal cell crosstalk improved human pluripotent stem cell derived CM (hPSC-CM) maturation. These systems have proven useful for modeling some types of cardiac disease and for drug screening (reviewed in Arslan et al., 2022). However, most of these models lacked functional vasculature as they were maintained in static cultures. In chapter 5, we developed a vascularized 3D cardiac microtissue on a chip (VMToC). We combined prevascularized hiPSC-derived 3D cardiac microtissues (MTs) and vascular cells (human induced pluripotent stem cell derived endothelial cells (hiPSC-EC) and human brain vascular pericytes (HBVP)) in a fibrin hydrogel in a commercial organ-on-chip culture platform. Vascular cells self-organized into an external vascular network which interconnected/anastomosed with the preexisting microvascular networks in the MTs. We showed that fluid flow was essential for the anastomosis which was enhanced by continuous perfusion. Here, we characterized VMToCs functionally. We first investigated whether vascularization affects parameters such as sarcomere organization and spontaneous or paced contraction. We showed that the sarcomere organization was not affected by the presence of vascular structures. However, contraction duration was significantly longer in VMToCs. Notably, we demonstrated that EC-CM crosstalk can be modeled in vascularized cardiac MT on chip (VMToC) cultures: by using either L-N-Nitro arginine methyl ester (L-NAME), an inhibitor of nitric oxide synthetases (NOS), or pro-inflammatory stimuli, such as interleukin-1β (IL-1β), we revealed some of the paracrine signals playing roles in the regulation of cardiac function in MTs.

Figure 1

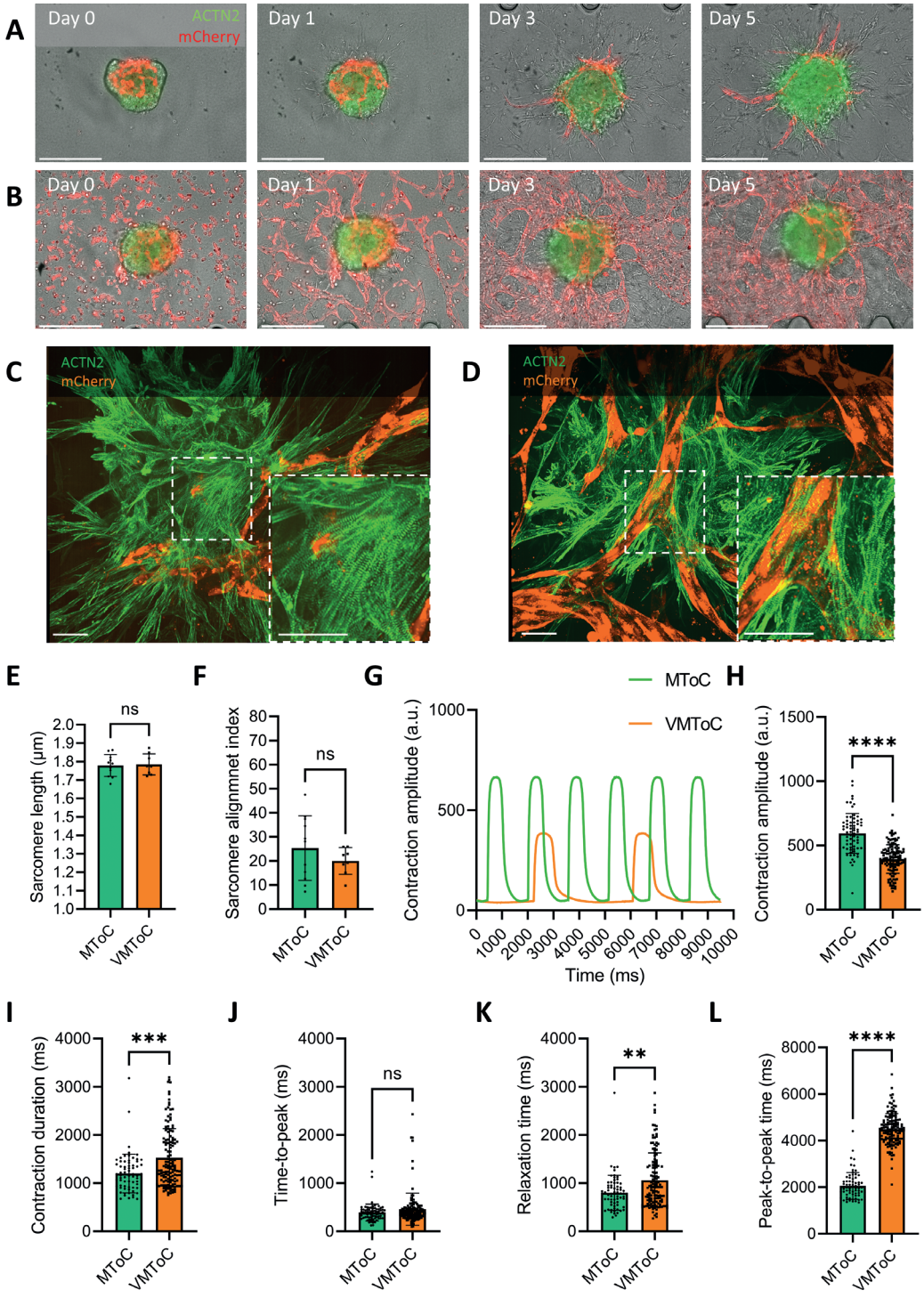

Figure 1: Characterization of contractile dynamics of cardiac MTs in MToC and VMToC. *(A, B) Representative images of MTs in chips on day 0, 1, 3 and 5 in MToC (A), and VMToC (B) (10×). Scale bar, 300 µm. (C, D)*

*Representative confocal images of sarcomeres showing hiPSC-ECs (orange, mCherry) and hiPSC-CM (green, ACTN2) in MToC (C) and VMToC (D) (40x). White dash box is the area that is zoomed 100x. Scale bar, 50 μm. (E, F) Quantification of the sarcomere parameters: sarcomere length (E); sarcomere alignment index (F); Error bars are shown as mean±SD from MToC N = 3, n = 11; VMToC N =4, n =8; three or four independent experiments with at least 8 MTs. (G) Representative beating traces of MTs from MToC (green trace) and VMToC (orange trace). (H-L) Quantification of the contraction parameters: contraction amplitude (H); contraction duration (I); time-to-peak (J); relaxation time (K); peak-to-peak time (L) in MTs with AICS-0075 hiPSC-CMs. Error bars are shown as mean±SD from MToC N = 3, n = 69; VMToC N =3, n=132; three independent experiments with 16 or 24 MTs from at least six different microfluidic channels each experiment. Student's t-test (E), Wilcoxon-Mann-Whitney test (F, and H-L). ***p < 0.001,****p < 0.0001; ns, not significant.*

Results

Characterization of cardiac MTs in the absence or presence of external vascular network

hiPSC-derived 3D cardiac microtissues (MTs) were formed using CMs, ECs, and CFs, as previously established (Campostrini et al., 2021). These MTs were maintained 12 days in static culture conditions and then integrated in AIM Biotech 3D cell culture chips. We examined cardiac MTs in the chips for any changes in their sarcomere organization and contractile properties. MTs were compared in the absence (MToC, 1A) or presence (VMToC, Figure 1B) of an external vascular network. Sarcomere morphologies appeared similar in the MToC (Figure 1C) and VMToC (Figure 1D) which was confirmed by similar sarcomere lengths (Figure 1E) and alignment indices (Figure 1F) assessed using the SOTATool (Stein et al., 2022). This indicated that there was no additional effect on sarcomere organization in the presence of an external vascular network. Contractility of cardiac MTs was analyzed using the video-based software tool MUSCLEMOTION (Sala et al., 2018). Representative beating traces showed that MTs under both conditions maintained their contractility in hydrogel (Figure 1G). However, contraction amplitude (Figure 1H) was significantly lower in VMToC, and contraction duration (Figure 1I), relaxation time (Figure 1K) and peak-to-peak time (Figure 1L) were significantly longer in VMToC. Time-to-peak (Figure 1J) was similar in both conditions.

The changes in these parameters were consistent in VMToC and MToC that were generated using a second, independent hiPSC line as a source of CMs (Figure 2A-E). In order to test whether the increase in contraction duration and relaxation time in the VMToC is not beat rate dependent, we electrically paced MTs in the chips using custom-made electrodes that fit the gel channel inlet and outlet. When the MTs were paced at 0.8 Hz and 1 Hz (Figure 2F-G), contraction duration at 90% and 50% transient was significantly higher in VMToC compared to MToC, consistent with the results under conditions of spontaneous beating (Figure 2H-I). We further investigated if the duration differences could be explained by time-to-peak or relaxation time changes. However, these parameters were highly variable and were not significantly different between VMToC and MToC even when paced (Figure 2J-K).

Figure 2

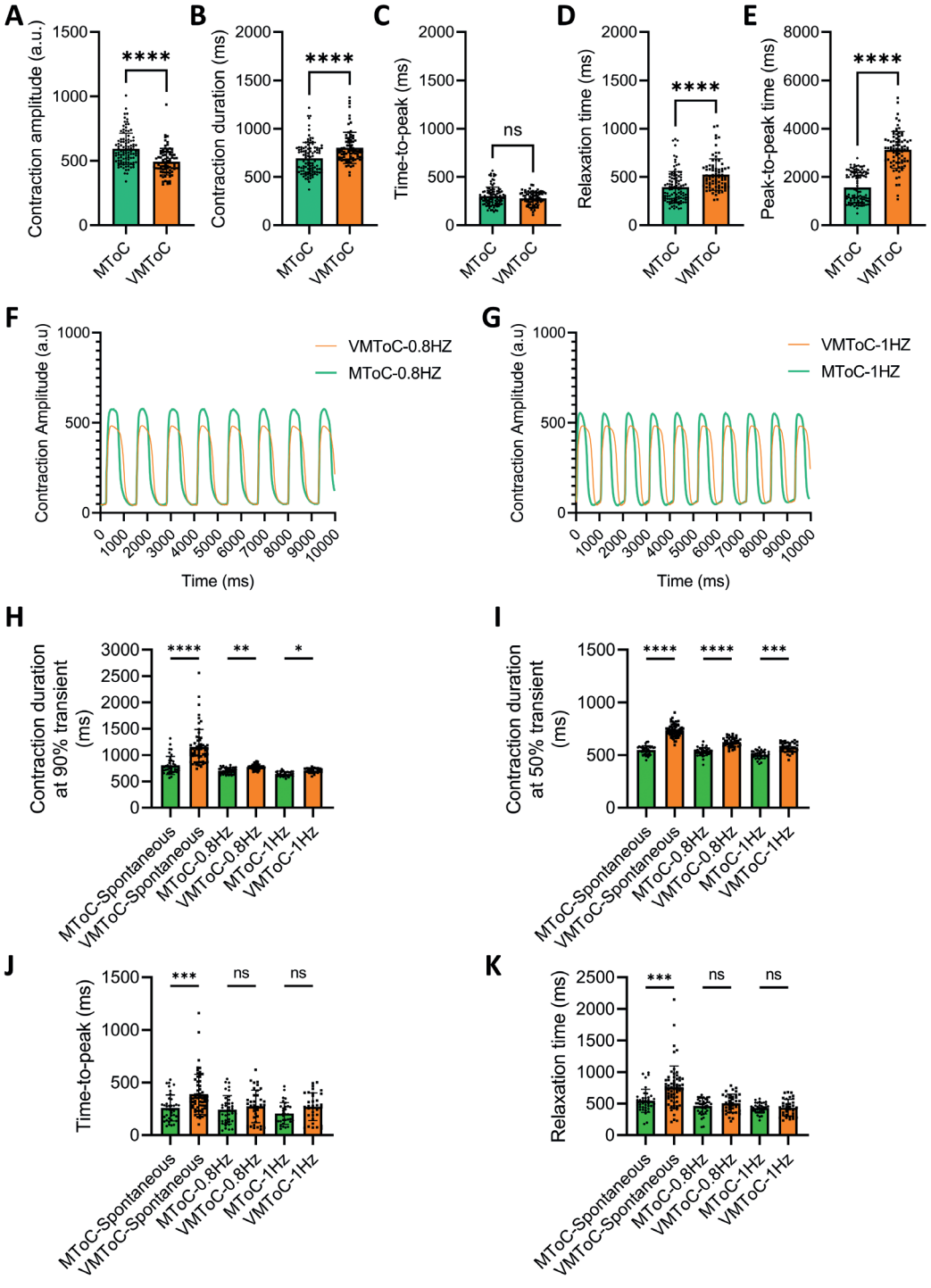

Figure 2: Characterization of contraction parameters upon pacing. *(A-E) Quantification of the contraction parameters of MToC and VMToC: contraction amplitude (A); contraction duration (B); time-to-peak (C);*

*relaxation time (D); peak-to-peak time (E) in MTs with LUMC0059iCTRL03 hiPSC-CMs. Error bars are shown as ±SD from MToC N = 3, n>30; VMToC N =3, n>26; three independent experiments with 26 MTs from at least six different microfluidic channels in each experiment. (F-G) Representative beating traces at 0.8 Hz (A) and 1 Hz (B). (H-K) Quantification of the contraction parameters during spontaneous beating, at 0.8 Hz and 1 Hz paced MTs: contraction duration at 90% transient (H); contraction duration at 50% transient (I); time-to-peak (J); relaxation time (K) in MTs with AICS-0075 hiPSC-CMs. Error bars are shown as ±SD from MToC N = 3, n >10; VMToC N =3, n>10; three independent experiments with 10 MTs from at least three different microfluidic channels were carried out for each experiment. Wilcoxon-Mann-Whitney test (A-E), Kruskal-Wallis test with Dunn's multiple comparisons test (H-K); *p < 0.05, **p < 0.01; ***p < 0.001, ****p < 0.0001; ns, not significant.*

Modeling EC-CM crosstalk in cardiac MTs

To explore whether VMToC have added value over MToC in studying inflammation, we investigated using two independent hiPSC lines for CMs whether EC-CM crosstalk can be modulated by either (1) L-NAME, a nonselective inhibitor of NOS or (2) pro-inflammatory stimuli, such as IL-1β. MToC and VMToC were incubated with L-NAME or vehicle for one hour (Figure 3A-D and 4A-D) or six hours (Figure 3E-H and 4E-H). L-NAME had no effect on the contraction time parameters: duration, time-to- peak and relaxation time in MToC after one- or six-hour incubation compared to the vehicle alone. By contrast, six-hour L-NAME exposure of VMToC cultures decreased contraction duration (Figure 3E, 4E) and relaxation time (Figure 3G, 4G) but had no effect on the time-to-peak (Figure 3F, 4F). One- hour of L-NAME incubation was more variable between the lines tested, and decreased contraction duration and relaxation time in one but not the other control line (Figure 3A, C and 4A, C). Peak-to- peak times appeared to decrease in one of the control lines tested after one and six hours, but not the other (Figure 3D, H and 4D, H).

Finally, MToC and VMToC were stimulated for twelve hours with IL-1β (10 ng/ml) to investigate the effect of pro-inflammatory cytokines. Pro-inflammatory cytokine release and contractile parameters were assessed. Stimulation with IL-1β resulted in significant upregulation of IL-6 (Figure 3I), IL-8 (Figure 3J) and cytokine chemoattractant protein 1 (MCP-1/CCL2, Figure 4K) in VMToC but not in MToC. In addition, IL-1β stimulation decreased contraction duration, relaxation time and peak-to- peak time in VMToC but had no effect on MToC (Figure 3L-O).

Figure 3

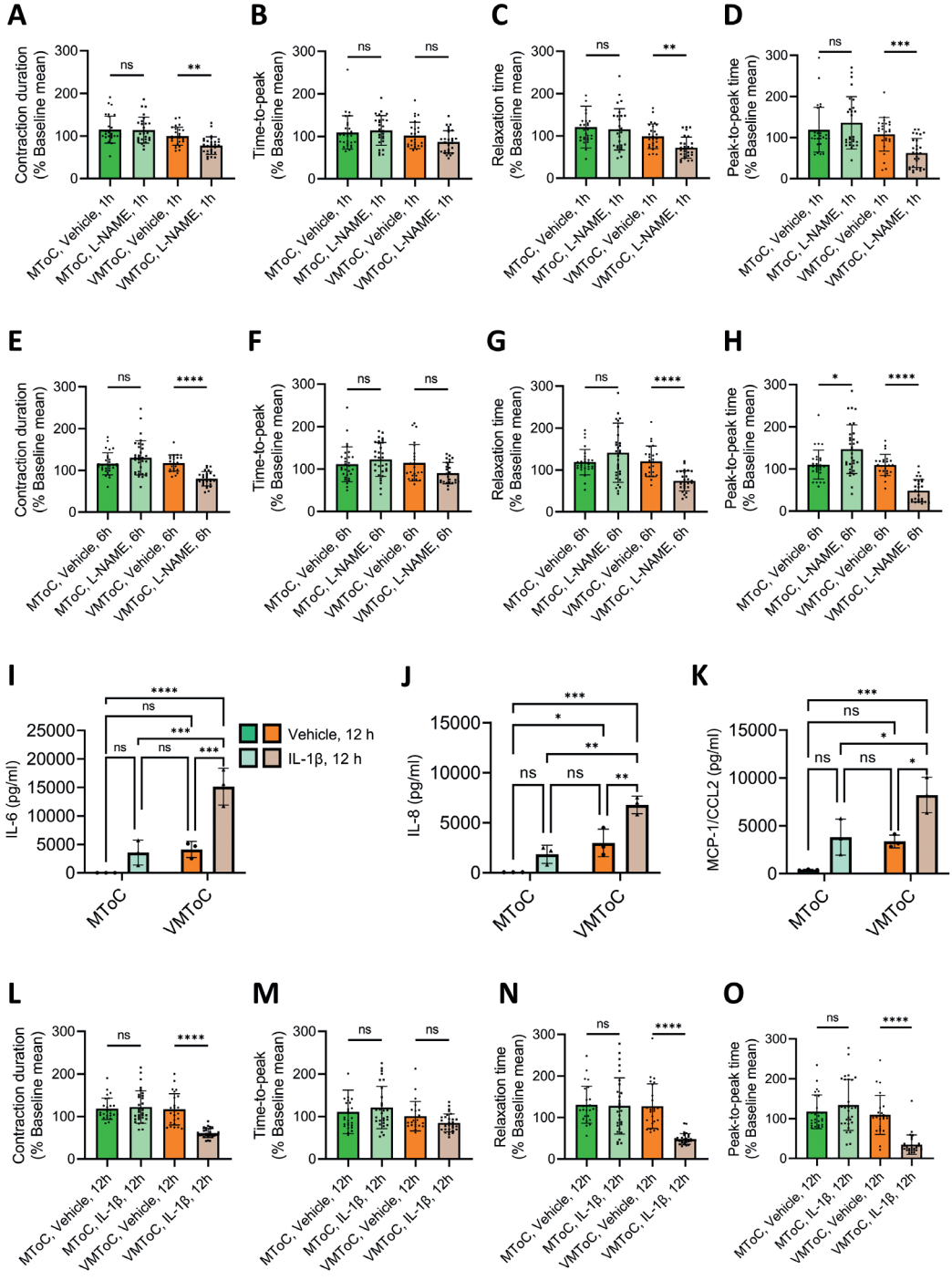

Figure 3: Altered contractile dynamics and inflammatory response of cardiac MTs regulated by EC- CM communication in VMToC but not in MToC. *(A-H) Quantification of the contraction parameters presented*

*as percentage change from the baseline mean of spontaneous beating condition, after 1 h (A-D) and 6 h (E-H) incubation with Vehicle or L-NAME (1 mM): contraction duration (A, E); time-to-peak (B, F); relaxation time (C, G); peak-to-peak time (D, H) in MTs with LUMC0059iCTRL03 hiPSC-CMs. Error bars are shown as mean±SD from MToC N = 3, n > 28 (Vehicle) and n > 27 (L-NAME); VMToC N =3, n > 24 (Vehicle) and n > 27 (L-NAME); three independent experiments with at least 7 MTs in each experiment. (I-K) Quantification of proinflammatory cytokines from the medium after 12 h incubation of IL-1β (10 ng/ml): IL-6 (I); IL-8 (J); MCP1/CCL2 (K) in MTs with LUMC0059iCTRL03 hiPSC-CMs. Y-axis shows concentration (pg/ml). Error bars are shown as mean±SD. MToC N = 3, n>3; VMToC N =3, n > 3; three independent experiments, medium was collected from at least with 3 different microfluidic channels in each experiment. (L-O) Quantification of the contraction parameters presented as percentage change from the baseline mean of spontaneous beating condition after 12 h incubation with Vehicle or IL-1β (10 ng/ml): contraction duration (L); time-to-peak (M); relaxation time (N); peak-to-peak time (O) in MTs with LUMC0059iCTRL03 hiPSC-CMs. Error bars are shown as mean±SD from MToC N = 3, n = 26 (Vehicle) and n = 30 (IL-1β); VMToC N =3, n = 25 (Vehicle) and n = 31 (IL-1β); three independent experiments with at least 7 MTs in each experiment. Kruskal-Wallis test with Dunn's multiple comparisons test (A-H, L-O), 2-way ANOVA with Šidák's multiple comparisons test (I- K), *p < 0.05, **p < 0.01, ***p < 0.001; ****p < 0.0001; ns, not significant.*

Discussion

In chapter 5, we developed a perfusable hiPSC-derived VMToC model. Here, we further characterized VMToCs in their function and EC-CM crosstalk. Previously we demonstrated that including ECs and cardiac fibroblasts (CFs) in MTs enhances CM maturation (Giacomelli et al, 2020). However, no differences in sarcomere organization were found between VMToC and MToC, indicating that further enhancement was not induced by the external vascular network. VMToCs showed characteristic low beat rates but nevertheless they continued to contract rhythmically throughout the experiments. Analysis of VMToC contractile parameters showed increased contraction duration and relaxation times. Notably, the increase in contraction duration in VMToC was not rate dependent and was maintained upon pacing at 0.8 and 1 Hz.

We further demonstrated that EC-CM crosstalk could be captured in VMToC upon delivery of stimuli via the external vascular network. Inhibition of NOS using L-NAME in VMToCs reversed the slow beating and decreased contraction duration, relaxation and peak-to-peak time. At the same time, L- NAME had no significant effect in MToC after one- or six hours incubation, except for an increase in peak-to-peak time. The effect of L-NAME in VMToC could be explained by a possible increase in endothelium-derived endothelin (ET-1) production upon NOS inhibition (Kourembanas et al., 1993; Czóbel et al., 2009). Since VMToCs contain more ECs than MToCs, this could result in a pronounced response to NOS inhibition that was not observed in MToCs. Similarly, stimulation with IL-1β for twelve hours resulted in upregulation of several pro-inflammatory cytokines, such as IL-6, IL-8 and MCP-1 in VMToC, but not in MToC, suggesting that only the vascular units were effectively responding to pro-inflammatory cytokine stimulation that are known contributors to EC dysfunction and heart failure. Stimulation with IL-1β decreased contraction duration, relaxation time and peak- to-peak time. This was somewhat unexpected since IL-1β and IL-6 are known as negative inotropes that increase NO levels via upregulating the expression of inducible NOS (iNOS) in isolated CMs (Segers et al., 2018). On the other hand, IL-1β and

Figure 4

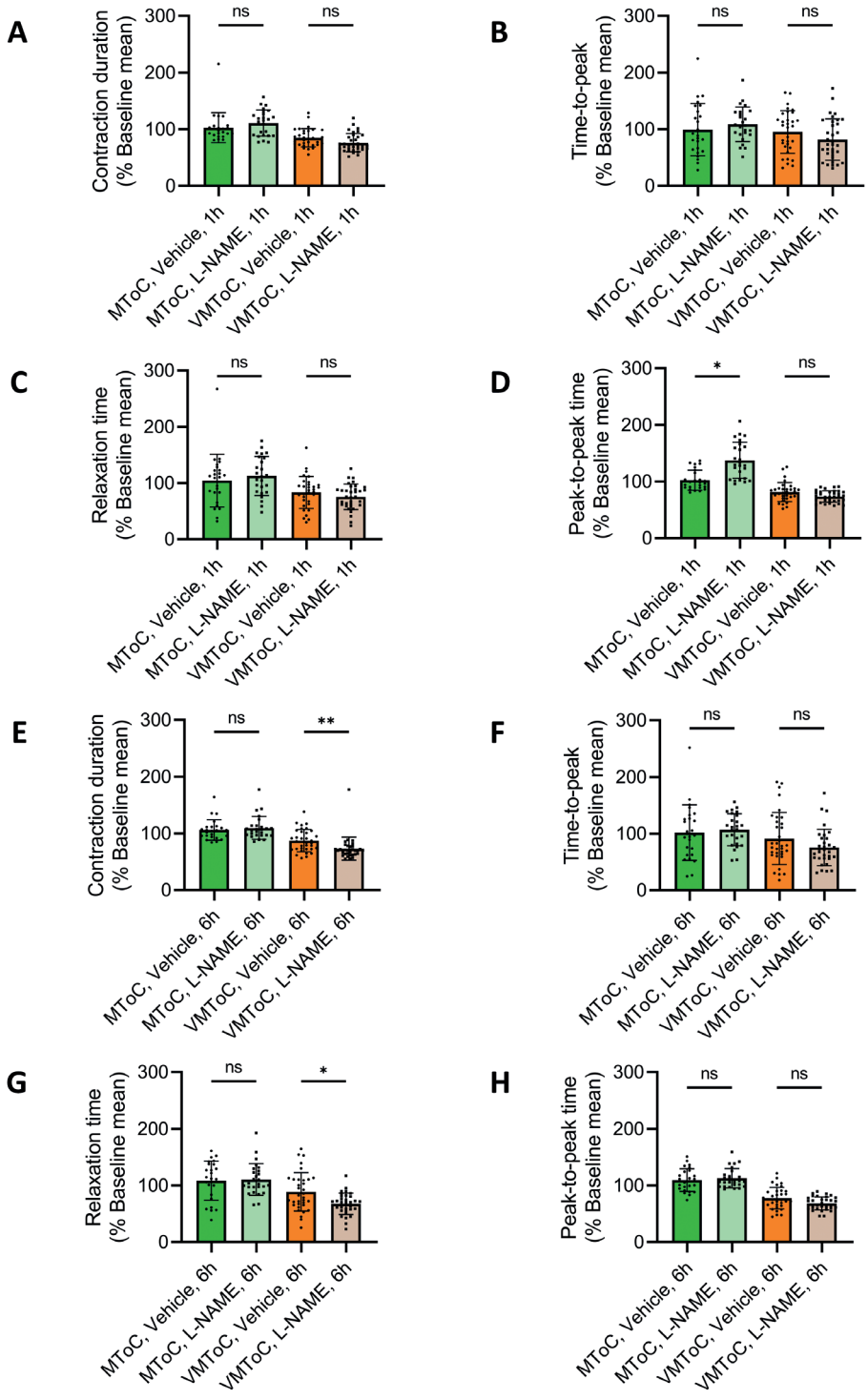

Figure 4: Altered contractile dynamics of cardiac MTs upon inhibition of EC-CM communication in VMToC but not in MToC, using a second control line. *(A-H) Quantification of the contraction parameters presented*

*as percentage change from the baseline mean of spontaneous beating condition, after 1 h (A-D) and 6 h (E-H) incubation of L-NAME (1 mM): contraction duration (A, E); time-to-peak (B, F); relaxation time (C, G); peak-to-peak time (D, H) in MTs with AICS-0075 hiPSC-CMs. Error bars are shown as ±SD from MToC N = 3, n >6; VMToC N =3, n > 7; three independent experiments with at least 6 MTs from at least four different microfluidic channels in each experiment. Data is normalized to baseline mean of each set for vehicle and L- NAME group of MTs. Kruskal-Wallis test with Dunn's multiple comparisons test (A-H). *p < 0.05, **p < 0.01; ns, not significant.*

IL-6 decrease endothelial NOS (eNOS) expression and activity in ECs (Saura et al., 2006; Kawasaki et al., 2015; Hung et al., 2010). Although we have not examined expression of iNOS and eNOS upon IL-1β treatment in VMToC vs MToC, the fact that the IL- 1β inhibitory effect was only observed in VMToC indicates the importance of the vascular component in mediating the response in CMs.

Finally, inter-batch and inter-line variability might be the result of differences in basal contractile parameters and/or drug responses in VMToCs. We showed consistency between two different hiPSC lines but further validation using more hiPSC lines may be of value as NOS levels may differ between CMs and ECs from different lines and thus affect contractile dynamics and drug responses to different extents.

In summary, we showed here that the presence of vasculature significantly affected the contraction time parameters of VMToC, However, the sarcomere organization was not affected by vascularization. We challenged EC-CM crosstalk in two ways: NOS inhibition and stimulation with a pro-inflammatory cytokine. As a result, pro-inflammatory cytokine concentration, contraction duration and peak-to-peak time significantly changed only in VMToC, but not in MToC. These results suggest that EC-CM crosstalk is enhanced in VMToC and regulated CM contraction and response to stimuli, highlighting the utility of VMToC.

Experimental Procedures

Detailed experimental procedures on hiPSC line maintenance, cardiac microtissue and cell preparation before on chip cultures can be found on chapter 5.

Microfluidic chip culture

Cells and MTs mixtures were seeded in commercially available microfluidic chips (AIM Biotech) as follows: 1) 4 MT/channel in combination with 25 × 106 hiPSC-ECs/mL and 5 × 106 HBVP cells/mL (5:1 ratio) (VMToC); or 2) 4 MT/channel (MToC) were resuspended in endothelial growth medium-2 (EGM-2, Lonza) supplemented with Thrombin (4 U/mL). This mixture was then added to fibrinogen (final concentration 3 mg/mL, Sigma) at 1:1 vol ratio and gently mixed. Final mixture was loaded into the middle gel-loading channel of the microfluidic chip. Chips were incubated at room temperature for 15 min. The chips were maintained in a medium mixture consists of (bovine serum albumin (BSA) and essential

lipids (B(P)EL) medium and endothelial growth medium-2 (EGM-2); 50:50), supplemented with vascular endothelial growth factor (VEGF) (50 ng/mL). On day 1, the γ-secretase inhibitor DAPT (10 µM) was added to the medium for 24 h. Intermittent gravity-driven flow in the whole chamber was induced by the addition of 100 µL medium to the right media ports and 50 µL media to left media ports in the medium channel which creates hydrostatic pressure. Medium was refreshed daily until day 7 and characterized between day 5-7.

L-NAME and IL-1β stimulation

On the day of L-NAME stimulation chips were refreshed with the medium supplemented with either VEGF (50 ng/mL) and distilled water (Vehicle) or VEGF (50 ng/mL) and L-NAME (1 mM, N5751, Sigma) for one or six hours. Chips were incubated at 37 °C, 5% CO2 and contraction analyses were performed after one hour or six hours.

On the day of IL-1β stimulation chips were refreshed with the medium supplemented with either VEGF (50 ng/mL) and PBS (Vehicle) or VEGF (50 ng/mL) and IL-1β (10 ng/ml, N5751, Sigma) for twelve hours. Chips were incubated at 37 °C, 5% CO2 and contraction analyses were performed after twelve hours.

Multiplex Cytokine Analysis

The medium from multiple chips were collected after twelve hours stimulation with IL-1β (10 ng/ml) or vehicle, and kept at -80 oC. On the day of the multiplex cytokine bead assay, collected medium was thawed two hours prior to the experiment. Concentration of cytokines (CXCL10, IL-1β, TNFα, CCL2, IL-6, IL-10, IFNϒ, TGFβ1 free active and IL-8) was measured using a LEGENDplex Human Essential Immune Response Panel kit (13-plex) (BioLegend, cat no: 740930) according to the manufacturer's instructions. Undiluted or eight times diluted samples were run on Cytek 3-Laser Aurora spectral flow cytometer (Cytek Biosciences, USA).

Imaging of vascularized 3D cardiac microtissues on chip

Whole channel images were captured daily using EVOSM7000 with 10x objectives. Confocal images were captured to create 3D stack using Andor Dragonfly spinning disk confocal microscope using a 40x objective. Images were processed using Imaris 9.5 software (Bitplane, Oxford Instruments).

Contraction analysis

For pacing experiments, electrodes were made in-house to fit to the gel channels of chips and used to pace MTs. MTs were stimulated at 0.8 and 1 Hz, with 15V/cm strength and 3 ms long stimulation pulse. Movies of spontaneous beating or paced MTs from VMToC and MToC

conditions were acquired for at least 10 s at 37 °C either with a ThorLabs DCC3240M camera at 100 frames/s and a 10x objective phase contrast objective (Leica Inverted microscope IBDE), using the ThorLabs uc480 software (v 4.20), or with a Leica Microsystems LAS AF6000 microscope at 37 °C and 5 % CO2. On the day of L-NAME or IL-1β stimulation, VMToC and MToC conditions were recorded for their baseline spontaneous beating prior to drug administration. Chips were recorded after both one hour incubation and six hours incubation period with vehicle and L-NAME or twelve hours incubation period with IL-1β. Contraction data were obtained by analyzing movies with the MUSCLEMOTION ImageJ macro (ImageJ v. 2.0.0-rc-49) as described previously (Sala et al., 2018).

Sarcomere analysis

Confocal images of VMToC and MToC conditions were acquired using a DragonFly spinning disk (Andor) microscope with 40x objective. In each MT, one plane from each FOVs were chosen to quantify and converted to 8-bit images. For MToC, 88 FOVs were selected in 11 MTs and for VMToC 52 FOVs were selected in 8 MTs. Sarcomere quantification data was obtained by analyzing these 8-bit images with SotaTool, as described previously (Stein et al., 2022).

Statistical analysis

Statistical analysis was performed using GraphPad Prism 9. Student's t-test, one-way or two-way ANOVA for paired or unpaired measurements were applied as appropriate to test for differences in means between groups/conditions. Kruskal–Wallis test and Wilcoxon-Mann-Whitney test were used when the normality assumption did not hold. Data are expressed and plotted as the Mean ± SD. as indicated in figure legend. Detailed statistics and exact P-values are indicated in each figure legend. Statistical significance was defined as $P < 0.05$.

References

Arslan, U., Moruzzi, A., Nowacka, J., Mummery, C. L., Eckardt, D., Loskill, P., and Orlova, V. V. 2022. *Microphysiological stem cell models of the human heart.* Materials Today Bio 14:100259.

Berry, C., and Duncker, D. J. 2020. *Coronary microvascular disease: The next frontier for Cardiovascular Research.* Cardiovascular Research 116(4):737-740.

Campostrini, G., Meraviglia, V., Giacomelli, E., van Helden, R. W. J., Yiangou, L., Davis, R. P., Bellin, M., Orlova, V. V., and Mummery, C. L. 2021. *Generation, functional analysis and applications of isogenic three-dimensional self-aggregating cardiac microtissues from human pluripotent stem cells.* Nature Protocols 16(4):2213-2256.

Czóbel, M., Kaszaki, J., Molnár, G., Nagy, S., and Boros, M. 2009. *Nonspecific inhibition of nitric oxide synthesis evokes endothelin-dependent increases in myocardial contractility.* Nitric Oxide - Biology and Chemistry 21(3-4):201-9.

Hung, M. J., Cherng, W. J., Hung, M. Y., Wu, H. T., and Pang, J. H. S. 2010. *Interleukin-6 inhibits endothelial nitric oxide synthase activation and increases endothelial nitric oxide synthase binding to stabilized caveolin-1 in human vascular endothelial cells.* Journal of Hypertension 28(5):940-51.

Kawasaki, Y., Yokobayashi, E., Sakamoto, K., Tenma, E., Takaki, H., Chiba, Y., Otashiro, T., Ishihara, M., Yonezawa, S., Sugiyama, A., et al. 2015. *Angiostatin prevents IL-1β-induced down-regulation of eNOS expression by inhibiting the NF-κB cascade.* Journal of Pharmacological Sciences 129(3):200-4.

Kourembanas, S., McQuillan, L. P., Leung, G. K., and Faller, D. V. 1993. *Nitric oxide regulates the expression of vasoconstrictors and growth factors by vascular endothelium under both normoxia and hypoxia.* Journal of Clinical Investigation 92(1):99-104.

Sala, L., van Meer, B. J., Tertoolen, L. G. J., Bakkers, J., Bellin, M., Davis, R. P., Denning, C., Dieben, M. A. E., Eschenhagen, T., Giacomelli, E., et al. 2018. *Musclemotion: A versatile open software tool to quantify cardiomyocyte and cardiac muscle contraction in vitro and in vivo.* Circulation Research 122(3):e5-e16.

Saura, M., Zaragoza, C., Bao, C., Herranz, B., Rodriguez-Puyol, M., and Lowenstein, C. J. 2006. *Stat3 mediates interelukin-6 inhibition of human endothelial nitric-oxide synthase expression.* Journal of Biological Chemistry 281(40):30057-62.

Segers, V. F. M., Brutsaert, D. L., and De Keulenaer, G. W. 2018. *Cardiac remodeling: Endothelial cells have more to say than just NO.* Frontiers in Physiology 9:382.

Stein, J. M., Arslan, U., Franken, M., De Greef, J. C., Harding, S. E., Mohammadi, N., Orlova, V. V, Bellin, M., Mummery, C. L., and Van Meer, B. J. 2022. *Software Tool for Automatic Quantification of Sarcomere Length and Organization in Fixed and Live 2D and 3D Muscle Cell Cultures In Vitro.* Current Protocols in Human Genetics 2(7):e462.